Journal of Science and Technology in Civil Engineering, HUCE, 2025, 19 (3): 38–53

NUMERICAL INVESTIGATION OF THE AXIAL COMPRESSIVE CAPACITY OF REINFORCED CONCRETE-FILLED DOUBLE-SKIN STEEL TUBULAR SHORT COLUMNS

Nguyen Van Ninh[a], Pham Tuan Dung[b], Vu Quang Viet[c], Zhengyi Kong[d], Pham Thai Hoan[e,*]

[a]*Faculty of Civil Engineering, Vietnam Maritime University, 484 Lach Tray street, Le Chan ward, Hai Phong City, Vietnam*
[b]*School of Engineering, University of Aberdeen, Fraser Noble Building, Kings College, Aberdeen, AB24 3UE, United Kingdom*
[c]*Faculty of Advanced Technology and Engineering, VNU Vietnam Japan University, My Dinh Campus, Luu Huu Phuoc Road, Tu Liem Ward, Hanoi, Vietnam*
[d]*Institute for Sustainable Built Environment, Heriot-Watt University, Edinburgh, United Kingdom*
[e]*Faculty of Building and Industrial Construction, Hanoi University of Civil Engineering, 55 Giai Phong road, Bach Mai ward, Hanoi, Vietnam*

Article history:
Received 26/02/2025, Revised 18/8/2025, Accepted 10/9/2025

Abstract

This study presents a numerical investigation into the axial compressive behavior of reinforced concrete-filled double-skin steel tubular (R-CFDST) columns. A finite element model (FEM) for R-CFDST columns was developed based on validated FE models of both reinforced concrete-filled steel tubular (R-CFST) columns and circular concrete-filled double-skin steel tubular (CFDST) columns. Using the proposed FE model, a comprehensive parametric study was conducted to evaluate the effects of longitudinal reinforcement ratio, geometric dimensions, and material properties on the ultimate axial strength of R-CFDST columns. The results show that increasing the longitudinal reinforcement ratio from 0% to 2.93% enhances the column's ultimate capacity by up to 17.91%, underscoring the critical role of rebar in enhancing column performance. Furthermore, existing design equations for predicting the ultimate strength of R-CFST and CFDST columns were reviewed and adapted for application to R-CFDST columns. The accuracy of these modified equations was validated against the FE results, and the most accurate formulation was recommended for the compressive design of R-CFDST columns under uniaxial loading.

Keywords: ultimate axial strength; R-CFDST; rebar; FEM; compressive design.

https://doi.org/10.31814/stce.huce2025-19(3)-04 © 2025 Hanoi University of Civil Engineering (HUCE)

1. Introduction

Concrete-filled steel tubular (CFST) columns are increasingly utilized in high-rise buildings, bridge piers, and other structures due to their efficient combination of steel tubes and concrete cores. By integrating the compressive strength of the concrete core with the confinement and tensile strength of the surrounding steel tube, CFST columns exhibit improved ultimate load capacity, enhanced ductility, and greater resistance to local buckling. Overall, the design and application of CFST columns are well established in major structural design standards, including Eurocode 4 [1], ACI 318-14 [2], and AISC 360-22 [3]. Additionally, experimental investigations into the structural behavior of CFST columns have been conducted by numerous researchers, including Gardner and Jacobson [4], Schneider [5], and Uy [6]. Subsequently, numerous studies have expanded on CFST column behavior through theoretical and numerical approaches. More recently, machine learning techniques have

*Corresponding author. *E-mail address:* hoanpt@huce.edu.vn (Hoan, P. T.)

been widely applied to the design of these columns [7–9], enabling the practical use of this powerful method in structural design.

However, modern structural demands - such as higher load-bearing capacity, reduced cross-sectional dimensions, lightweight designs, and slender configurations - have driven research toward advanced enhancements of CFST columns. One such enhancement involves replacing the concrete near the neutral axis with a hollow steel tube, leading to the development of concrete-filled double-skin steel tubular (CFDST) columns. A CFDST column consists of an inner steel tube, an outer steel tube, and concrete infill confined within the annular space between them. Compared to traditional CFST columns, CFDST columns exhibit superior performance, including increased moment of inertia, enhanced structural stability, and improved ultimate strength under axial compression. The dual steel tubes provide better confinement for the concrete, enhancing its compressive strength while improving the strength-to-weight ratio.

Extensive theoretical and experimental studies [10–13] have examined the performance of CFDST columns, indicating that inadequate bond strength between the concrete core and steel tubes is a primary failure mechanism. This phenomenon is attributed to differences in expansion rates between concrete and steel during the elastic stage, as the Poisson's ratio of concrete is lower than that of steel.

Strengthening CFDST columns by incorporating longitudinal reinforcement within the concrete core has been shown to enhance deformation capacity and improve ultimate strength under axial compression. However, research on longitudinally reinforced CFDST columns remains limited. Furthermore, existing design standards, such as ACI 318-14 [2], Eurocode 4 [1] and AISC 360-22 [3], along with theoretical models proposed by several researchers [13–16], do not fully consider the influence of longitudinal reinforcing bars in CFDST columns. Most available formulations were developed for CFST columns. Therefore, this study aims to address this gap by investigating the compressive behavior of longitudinally reinforced CFDST short columns through a numerical approach. Fig. 1 presents a schematic of the longitudinally reinforced CFDST (R-CFDST) columns used in this study.

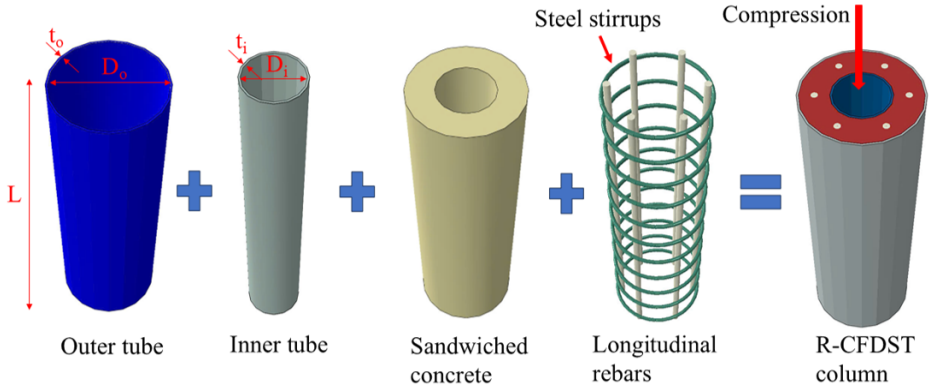

Figure 1. Sketch of longitudinally R-CFDST columns

The research methodology involves developing FE models for CFST and CFDST columns subjected to axial loading and validating them against experimental data. Using the same modelling procedure, a validated FE model is then developed for R-CFDST columns. Subsequently, a parametric study is carried out to explore the effects of longitudinal reinforcement ratio, steel tube geometry, and confinement conditions. The simulated results are compared with modified theoretical models to evaluate their accuracy and applicability for R-CFDST columns.

2. Calculation method for the ultimate capacity of R-CFDST columns

2.1. Existing design formulations for the ultimate capacity of CFDST columns

a. ACI 318-14

The ultimate load of CFDST columns under concentric axial compression is determined using a modified version of the equation for CFST columns, as specified in ACI 318-14 [2], as follows:

$$P_{u,ACI} = f_{syo}A_{so} + f_{syi}A_{si} + 0.85f_cA_c \tag{1}$$

where f_{syo} and f_{syi} are the yield strengths of the outer and inner steel tubes, respectively; f_c is the compressive strength of the concrete cylinder; A_{so}, A_{si}, and A_c are the cross-sectional areas of the outer and inner steel tubes, and concrete infill, respectively.

b. Eurocode 4

To calculate the ultimate load of CFDST columns under axial compression, Pagoulatou et al. [16] proposed an expression that incorporates the contribution of the inner steel tube based on the original formula for CFST columns in Eurocode 4 [1], as follows:

$$P_{u,EC4} = \eta_a\left(f_{syo}A_{so} + f_{syi}A_{si}\right) + f_cA_c\left[1 + \eta_c\left(\frac{t_o}{D_o}\right)\left(\frac{f_{syo}}{f_c}\right)\right] \tag{2}$$

in which, η_a is the reduction factor for the load-bearing capacity of the steel tube cross-section; and η_c is the enhancement factor for the concrete core, defined as follows:

$$\eta_a = 0.25(3 + 2\bar{\lambda}), \quad (\leq 1.0) \tag{3}$$

$$\eta_c = 4.9 - 18.5\bar{\lambda} + 17\,\bar{\lambda}^2, \quad (\geq 0) \tag{4}$$

in which $\bar{\lambda}$ is the slenderness ratio of the compressed column, determined as follows:

$$\bar{\lambda} = \sqrt{\frac{P_{pl,Rd}}{P_{cr}}} \tag{5}$$

where $P_{pl,Rd}$ is the characteristic plastic resistance, determined according to Eurocode 4 as follows:

$$P_{pl,Rd} = f_{syo}A_{so} + f_cA_c + f_{syi}A_{si} \tag{6}$$

P_{cr} is the elastic ultimate load for the corresponding buckling mode, defined as:

$$P_{cr} = \frac{\pi^2(EI)_{eff}}{(KL)^2} \tag{7}$$

Here, K is the effective length factor depending on the boundary conditions at the column ends (for clamped–guided conditions, K can be taken as 0.7), L is the column length, and EI_{eff} is the effective flexural stiffness of the composite section, calculated as follows:

$$(EI)_{eff} = E_{so}I_{so} + K_cE_{cm}I_c + E_{si}I_{si} \tag{8}$$

where K_c is a correcting coefficient that should be taken 0.6.

The elastic modulus of concrete could be determined by the following empirical expression provided by ACI 318-14 [2]:

$$E_{cm} = 4700\sqrt{f_c'} \tag{9}$$

c. AISC 360-22

The calculation of the ultimate load of CFDST columns under axial compression was modified based on that of CFST columns according to AISC 360-22 [3] as follows:

$$P_{u,AISC} = \begin{cases} P_p & \text{(compact)} \\ P_p - \dfrac{P_p - P_y}{\left(\lambda_r - \lambda_p\right)^2}\left(\lambda - \lambda_p\right)^2 + A_{si} f_{syi} & \text{(non-compact)} \\ P_y & \text{(slender)} \end{cases} \tag{10}$$

in which

$$P_p = A_{so} f_{syo} + 0.95 A_c f_c' + A_{si} f_{syi} \tag{11}$$

$$P_y = A_{so} f_{syo} + 0.7 A_c f_c' + A_{si} f_{syi} \tag{12}$$

$$f_{cr} = \frac{0.72 f_{syo}}{\left[\left(\frac{D_o}{t_o}\right)\frac{f_{syo}}{E_o}\right]^{0.2}} \tag{13}$$

d. Han et al. [17]

Han et al. [17] proposed a formula for calculating the ultimate load of CFDST columns, which includes two components: the load-bearing capacity of the inner steel tube and the combined load-bearing capacity of the outer steel tube and the concrete core, as follows:

$$(P_u)_{Han\ et\ al.} = P_{osc,u} + P_{i,u} \tag{14}$$

where $P_{i,u}$ is the load-bearing capacity of the inner steel tube, determined as:

$$P_{i,u} = f_{syi} A_{si} \tag{15}$$

and $P_{osc,u}$ is the combined load-bearing capacity of the outer steel tube and the concrete core:

$$P_{osc,u} = f_{osc} A_{soc} \tag{16}$$

where f_{osc} is the characteristic strength provided by the outer steel tube and the concrete core:

$$f_{osc} = C_1 \chi^2 f_{syo} + C_2 (1.14 + 1.02\xi) f_c \tag{17}$$

and C_1 is the strength coefficient of the outer steel tube, determined by the expression:

$$C_1 = \frac{\alpha}{1 + \alpha} \tag{18}$$

where α is calculated as:

$$\alpha = \frac{A_{so}}{A_c} \tag{19}$$

and χ is the hollow ratio of the cross-section of the CFDST column:

$$\chi = \frac{D_i}{D_o - 2t_o} \tag{20}$$

C_2 is the coefficient of strength for the concrete annulus, determined by the expression:

$$C_2 = \frac{1 + \alpha_n}{1 + \alpha} \tag{21}$$

where α_n is calculated as:

$$\alpha_n = \frac{A_{so}}{A_{c,no\,\min al}} \tag{22}$$

and ξ is the nominal confinement coefficient of the concrete, determined as:

$$\xi = \frac{f_{syo}A_{so}}{f_c A_{c,no\,\min al}} \tag{23}$$

where f_c is the characteristic compressive strength of the concrete, which can be determined from the cube compressive strength f_{cu} [17]

$$f_c = 0.67 f_{cu} \tag{24}$$

$A_{c,nominal}$ is the nominal cross-sectional area, calculated as:

$$A_{c,no\,\min al} = \frac{\pi(D_o - 2t_o)^2}{4} \tag{25}$$

A_{soc} is the summation cross-sectional area of the column, determined as:

$$A_{soc} = A_{so} + A_c \tag{26}$$

e. Yu et al. [14]

Yu et al. [14] proposed an empirical formula for determining the ultimate load of CFST columns as follows:

$$P_u = \left(1 + 0.5\frac{\xi}{1 + \xi}\Omega\right)\left(f_{sy}A_{st} + f_{ck}A_c\right) \tag{27}$$

where ξ is the concrete confinement coefficient, defined as:

$$\xi = \frac{f_{syo}A_{so}}{f_{ck}A_c} \tag{28}$$

and Ω is the solid ratio:

$$\Omega = \frac{A_c}{A_c + A_k} \tag{29}$$

in which A_k is the cross-sectional area of the hollow part.

Subsequently, Hassanein and Kharoob [18] modified the model proposed by Yu et al. [14] for application to CFDST columns subjected to axial compression, as follows:

$$(P_u)_{Yu\,et\,al.} = \left(1 + 0.5\frac{\xi}{1 + \xi}\Omega\right)\left(f_{syo}A_{so} + f_c A_c\right) + P_{i,u} \tag{30}$$

f. Hassanein et al. [15]

Hassanein et al. [15] proposed a model for determining the ultimate load of short CFDST columns with a circular cross-section under axial compression, as follows:

$$(P_u)_{Hassanein\,et\,al.} = \gamma_{so} f_{syo} A_{so} + \left(\gamma_c f_c + 4.1 f'_{rp,so}\right) A_c + \gamma_{si} f_{syi} A_{si} \tag{31}$$

where γ_{so} is the coefficient used to explain the strain-hardening effect on the outer steel, determined by the expression:

$$\gamma_{so} = 1.458\left(\frac{D_o}{t_o}\right)^{-0.1} \qquad (0.9 \le \gamma_{so} \le 1.1) \tag{32}$$

with γ_c being the intensity reduction factor of the concrete, proposed by Liang [19] as:

$$\gamma_c = 1.85 D_c^{-0.135}; \qquad 0.85 \le \gamma_c \le 1.0 \tag{33}$$

D_c is the diameter of the confined concrete core, determined as:

$$D_c = D_o - 2t_o \tag{34}$$

and $f'_{rp,so}$ is the lateral stress in the column:

$$f'_{rp,so} = \begin{cases} 0.7(v_o - v_s)\dfrac{2t_o}{D_o - 2t_o} f_{syo} & \left(\dfrac{D_o}{t_o} \le 47\right) \\ \left(0.006241 - 0.0000357\dfrac{D_o}{t_o}\right) f_{syo} & \left(47 < \dfrac{D_o}{t_o} < 150\right) \end{cases} \tag{35}$$

where v_o is the Poisson's ratio of the concrete-filled steel tube column, as proposed by Tang et al. [20]:

$$v_o = 0.2312 + 0.3582 v'_o - 0.1524\left(\frac{f_c}{f_{syo}}\right) + 4.843 v'_o\left(\frac{f_c}{f_{syo}}\right) - 9.169\left(\frac{f_c}{f_{syo}}\right)^2 \tag{36}$$

$$v'_o = 0.881 \times 10^{-6}\left(\frac{D_o}{t_o}\right)^3 - 2.58 \times 10^{-4}\left(\frac{D_o}{t_o}\right)^2 + 1.953 \times 10^{-2}\left(\frac{D_o}{t_o}\right) + 0.4011 \tag{37}$$

v_s is the Poisson's ratio of the steel tube at the maximum load-carrying capacity, typically taken as 0.5. γ_{si} is the coefficient used to explain the strain hardening effect on the inner steel, determined by the expression:

$$\gamma_{si} = 1.458\left(\frac{D_i}{t_i}\right)^{-0.1} \qquad (0.9 \le \gamma_{si} \le 1.1) \tag{38}$$

2.2. Design equations for the ultimate capacity of R-CFDST columns

In general, the standards ACI 318-14, Eurocode 4, and AISC 360-22 all provide guidance for calculating the ultimate load of CFST columns under axial compression, considering the contribution of longitudinal reinforcing bars. In contrast, many empirical models developed in previous studies for R-CFDST columns do not consider this effect. Therefore, to accurately evaluate the performance of these models, it is recommended to incorporate the contribution of longitudinal reinforcing bars into the ultimate load calculations for R-CFDST columns. In this study, this contribution is included by adding the term $A_s f_{sd}$ to the design models proposed by previous authors. A summary of all the formulas used to determine the ultimate load of R-CFDST columns (for compact sections only) from both design standards and existing studies is presented in Table 1.

Table 1. Summary of ultimate strength formulas for R-CFDST columns

No.	Design codes/ Empirical models	Design equations
1	ACI 318-14 [2]	$P_{u,ACI} = f_{syo}A_{so} + 0.85f_cA_c + f_{syi}A_{si} + A_sf_{sd}$
2	Eurocode 4 [1]	$P_{u,EC4} = \eta_a\left(f_{syo}A_{so} + f_{syi}A_{si}\right) + f_cA_c\left[1 + \eta_c\left(\frac{t_o}{D_o}\right)\left(\frac{f_{syo}}{f_c}\right)\right] + f_{sd}A_s$
3	AISC 360-22 [3]	$P_o = f_{syo}A_{so} + 0.95f_c\left(A_c + A_s\frac{E_s}{E_c}\right) + f_{syi}A_{si}$
4	Han et al. [17]	$(P_u)_{Han\,et\,al.} = P_{osc,u} + P_{i,u} + A_sf_{sd}$
5	Yu et al. [14]	$(P_u)_{Yu\,et\,al.} = \left(1 + 0.5\frac{\xi}{1+\xi}\Omega\right)\left(f_{syo}A_{so} + f_cA_c\right) + P_{i,u} + A_sf_{sd}$
6	Hassanein et al. [15]	$(P_u)_{Hassanein\,et\,al.} = \gamma_{so}f_{syo}A_{so} + \left(\gamma_cf_c + 4.1f'_{rp,so}\right)A_c + \gamma_{si}f_{syi}A_{si} + A_sf_{sd}$

It is noted that f_{sd} and A_s are the yield strength and the cross-sectional area of the longitudinal reinforcing bars, respectively.

3. Finite element model for reinforced circular CFDST columns

To evaluate the accuracy and effectiveness of design guidelines and theoretical models for circular CFDST columns reinforced with longitudinal reinforcing bars under axial compression, this study develops FE models that replicate previous experiments on reinforced CFST and CFDST columns. Subsequently, an FE model of R-CFDST columns with similar boundary conditions and simulation techniques is developed to analyze a series of columns with varying geometric dimensions, longitudinal reinforcement ratios, and material properties.

3.1. Finite element model (FEM)

The FEM was constructed using ABAQUS commercial software to simulate the behavior of reinforced circular CFDST columns under uniaxial compression. However, experimental studies on the axial behavior of reinforced circular CFDST columns with longitudinal steel reinforcement remain very limited. Therefore, this study initially developed FE models for the CFST, R-CFST, and the CFDST columns (without longitudinal reinforcement). The FE results were validated by comparison with experimental data reported in the literature. Subsequently, an FE model for the R-CFDST column with longitudinal reinforcing bars was developed, following the same modeling techniques and procedures.

In terms of material modeling, the study employs a bilinear elastoplastic stress-strain relationship to simulate the behavior of steel tube and reinforcing bar materials. The Young's modulus (E_s) and Poisson's ratio (μ) are set at 200 GPa and 0.3, respectively.

For the concrete infill, the stress-strain relationship proposed by Han et al. [21] is adopted to simulate concrete behavior, as defined by the following expression:

$$y = \begin{cases} 2x - x^2 & (x \le 1) \\ \dfrac{x}{\beta_o(x-1)^\eta + x} & (x > 1) \end{cases} \tag{39}$$

in which: $x = \dfrac{\epsilon}{\epsilon_0}; y = \dfrac{f}{f_c}$ represent the normalised strain and stress of concrete under axial compression; f_c is the cylinder compressive strength of concrete, and ϵ_0 is the axial strain corresponding to f_c.

The parameters η and β_0 are related to the cross-sectional shape of the column. This study focuses on the columns with circular sections, η is taken as 2 and the β_0 is defined as follows:

$$\beta_0 = 0.5\left(2.36 \times 10^{-5}\right)^{\left[0.25+(\xi-0.5)^7\right]}(f'_c)^{0.5} \geq 0.12 \tag{40}$$

where ξ is the nominal confinement factor of concrete, calculated based on [21].

The Poisson's ratio for concrete is taken as 0.2, and the concrete's modulus of elasticity is determined according to ACI 318-14 [2].

The Drucker-Prager model in ABAQUS is selected to simulate concrete failure. The friction angle, stress transfer ratio (K), and dilation angle for concrete are set to 20°, 0.8, and 30°, respectively [16, 22, 23].

Due to the relatively small thickness of the steel tube, the 4-node quadrilateral shell element (S4R) is used to model both the inner and outer steel tubes. The confining concrete is simulated using the 8-node linear brick element (C3D8R) [10, 16, 24], while the reinforcing bars are modeled using the truss element (T3D2). To determine a suitable mesh size for the components of the R-CFDST column, a sensitivity analysis is conducted using mesh sizes of 50 mm, 25 mm, 15 mm, and 10 mm for all components. Fig. 2 presents the influence of mesh size on the column capacity. The results show that mesh size has only a slight effect on the capacity. Specifically, the capacity decreases by approximately 5.2% when the mesh size is reduced from 50 mm to 15 mm, and remains almost unchanged when further reduced to 10 mm. Therefore, to save computational time, a mesh size of 15 mm is selected for all components. This choice also falls within the range of mesh sizes recommended for similar CFDST stub columns in the previous study [16].

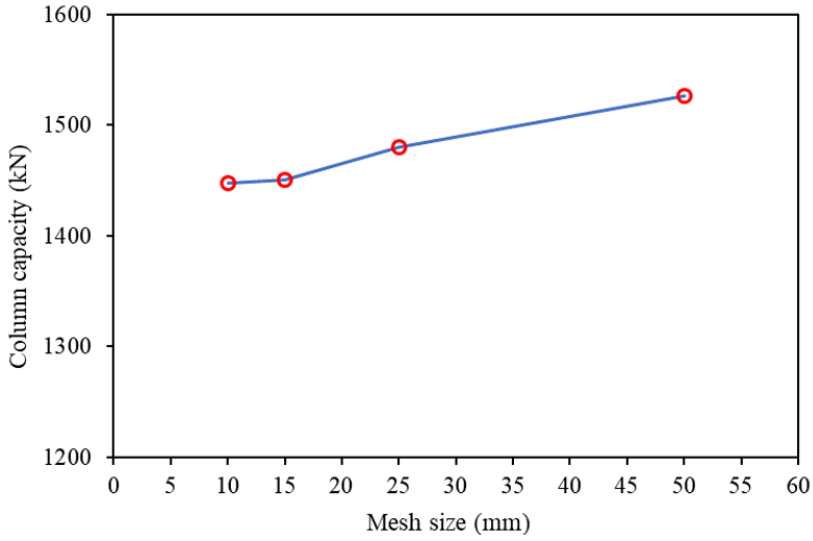

Figure 2. A sensitivity analysis for determining a suitable mesh size for R-CFDST columns

To define the interaction between components, a "surface-to-surface" contact approach is adopted to describe the interface between the inner and outer steel tubes and the concrete. In this model, the contact surface of the steel tube is designated as the master surface, while the concrete's contact surface is assigned as the slave surface. In ABAQUS, the master surface has higher stiffness during deformation and can penetrate the slave surface. The implemented contact type is hard contact, combined with penalty friction, with a friction coefficient of 0.6 [25–27].

The reinforcement bars are embedded directly within the concrete core using the "Embedded Region" method. Additionally, two reference points (RPs) are defined at the centroid of the bottom and top cross-sections of the column. A rigid body constraint links these reference points to their respective cross-sections, ensuring that the cross-sections remain flat during the analysis and thereby simulating the behavior of the loading plate used in experimental setup.

Boundary conditions are directly applied to these reference points. At the bottom cross-section, a fixed boundary condition is assigned to RP-1, while at the top cross-section, RP-2 is allowed to move only in the axial direction. To apply the increasing load, a direct axial displacement is imposed on RP-2. Fig. 3 presents FE models of R-CFST, CFDST, and R-CFDST columns used in this study.

(a) FE models of R-CFST columns (b) FE models of R-CFST columns (c) FE models of R-CDFST columns

Figure 3. FE models of R-CFST, CFDST, and R-CFDST columns

3.2. Verification of FE models of R-CFST and CFDST columns

The experiments on R-CFST and CFDST columns under uniaxial compressive loading, conducted by Xiamuxi et al. [28], Tao et al. [29], Ekmekyapar et al. [30], and Ekmekyapar and Hasan [31] were selected to validate the accuracy of the FE models. Table 2 and Fig. 4 present a comparison between the ultimate loads obtained from the FE models of CFST, R-CFST, and CFDST columns and the corresponding experimental results. It can be observed that the ultimate loads predicted by the FE models closely match the experimental values across all column types. As illustrated in Fig. 4, the R-squared value of 0.9736 indicates a strong correlation between the experimental data and the predicted ultimate loads. Additionally, a comparison of the axial load–displacement responses obtained from experimental results and FE simulations for specimens '0-2-1-1' and '0-2-2-2' [30] is shown in Fig. 5. Although discrepancies still exist between the FE and experimental results—arising from factors such as testing conditions, material uncertainties, and geometric tolerances—these differences are within an acceptable range. Based on these observations, it can be concluded that the developed FE model can accurately predict the ultimate load of columns with and without longitudinal reinforcing bars. Therefore, this modeling procedure is reliable and can be used for modeling R-CFDST columns under uniaxial compression.

Table 2. Comparison of the ultimate loads between the FE and test results for CFST, R-CFST, and CFDST columns

Specimen	Dimensions							Material properties			$P_{u,EXP}$ (kN)	$P_{u,FE}$ (kN)	$P_{u,FE}/P_{u,EXP}$	Type
	D_o (mm)	t_o (mm)	D_o/t_o	D_i (mm)	t_i (mm)	D_i/t_i	L (mm)	f_c (MPa)	f_{yo} (MPa)	f_{yi} (MPa)				
CF [28]	219	2.75	79.6	-	-	-	600	31.8	284	-	2036.6	1918	0.942	CFST
RF132 [28]	219	2.75	79.6	-	-	-	600	31.8	284	-	2448	2253.6	0.921	R-CFST
cc3a [29]	180	3	60	88	3	29.33	540	47.4	275.9	370.2	1631.7	1633.3	1.001	CFDST
cc6a [29]	240	3.0	60	114	3	38	720	47.4	275.9	294.5	2421	2520	1.041	
0-2-1-1 [30]	114.3	2.74	41.7	60.3	5.77	10.5	343	42.87	355	310	969.1	943.5	0.974	
0-2-1-2 [30]	114.3	6.11	18.7	60.3	5.77	10.5	343	42.87	535	310	1823.4	1715.0	0.941	
0-1-2-1 [30]	114.3	2.74	41.7	60.3	2.52	23.9	343	71.02	355	396	914.3	991.1	1.084	
0-2-2-2 [30]	114.3	6.11	18.7	60.3	5.77	10.5	343	71.02	535	310	1889.7	1816.5	0.961	
1-1-2 [31]	114.3	5.85	19.5	60.3	2.52	23.9	343	40.24	455	396	1419.1	1311.2	0.924	
2-1-1 [31]	114.3	2.73	41.9	60.3	5.77	10.5	343	40.24	285	310	910.8	842.4	0.925	
2-1-2 [31]	114.3	5.85	19.5	60.3	5.77	10.5	343	40.24	455	310	1576.8	1436.4	0.911	
						Mean							0.966	

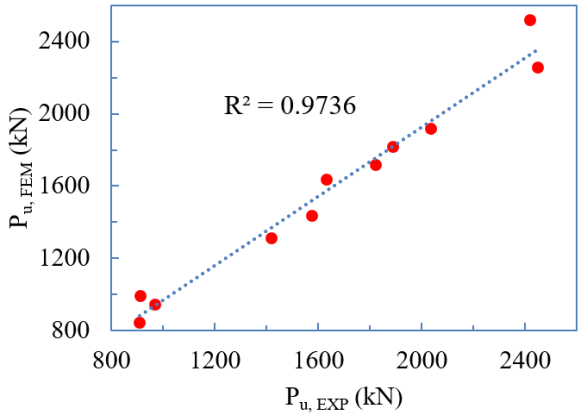

Figure 4. Comparison of ultimate compressive strength between test results and FE simulations

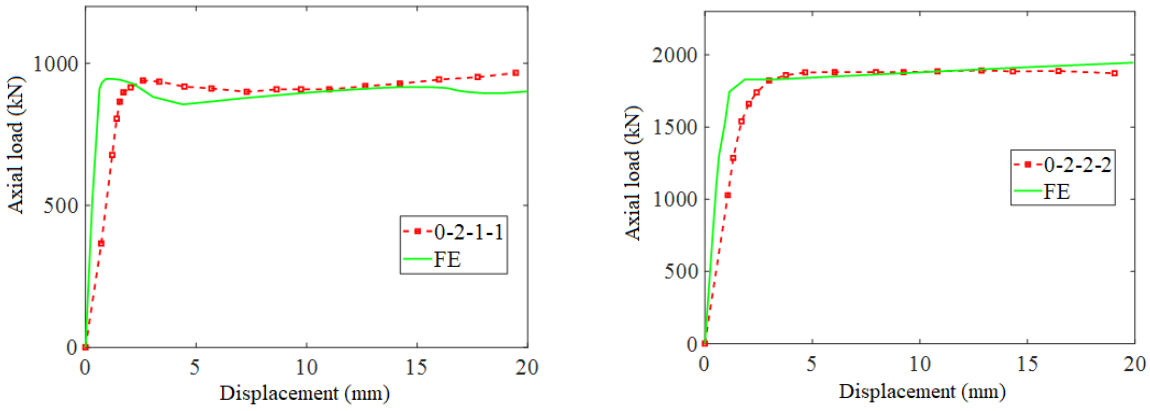

(a) Specimen 0-2-1-1 [30] (b) Specimen 0-2-2-2 [30]

Figure 5. Comparison of load – displacement response between experiment and FE results

4. Effect of structural parameters on the compressive capacity of R-CFDST columns

This section aims to investigate the effects of geometric dimensions, material properties, and longitudinal reinforcement ratio on the capacity of R-CFDST columns under compression. The FE models of R-CFDST columns were developed based on the validated modeling procedure in Section 3 to examine these effects. All considered case studies are presented in Table 3, while the effects of parameters, including longitudinal reinforcement ratio, concrete compressive strength, yield strengths of the inner and outer steel tubes, and column hollow ratio, are illustrated in Figs. 6–10.

To investigate the influence of the longitudinal reinforcement ratio on the R-CFDST column capacity, this ratio is varied from 0% (no rebar) to 0.73%, 1.3%, 2.04%, and 2.93% (using six rebars of a diameter of 12), while other parameters are fixed. It can be seen from Fig. 6 that the longitudinal reinforcement ratio has a significant impact on the column capacity. Especially, when this ratio increases from 0% to 2.93%, the column capacity remarkably increases by up to 17.91%, highlighting the importance of longitudinal reinforcement in the concrete core.

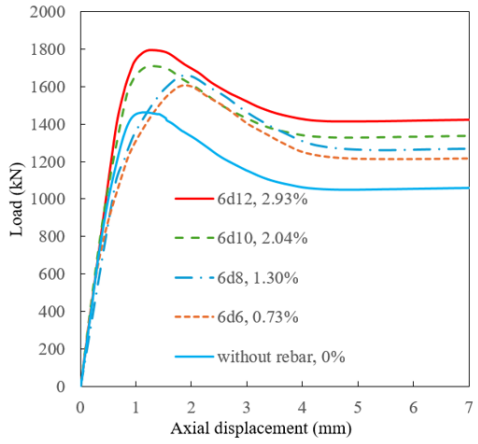

Figure 6. Influence of longitudinal reinforcement ratio on the column capacity

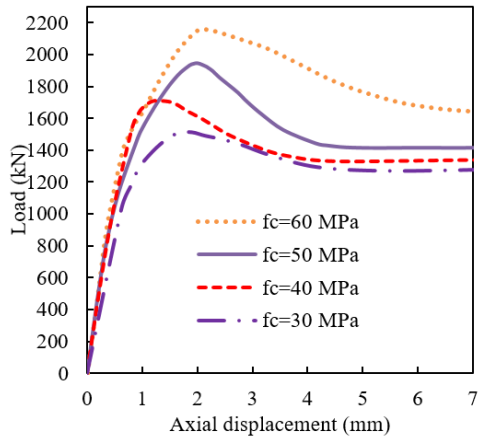

Figure 7. Influence of concrete compressive strength on the column capacity

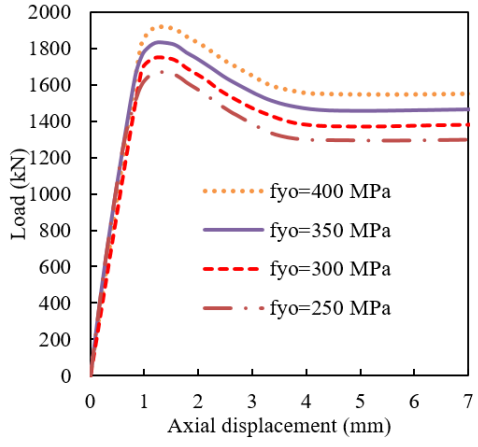

Figure 8. Influence of outer tube yield strength on the column capacity

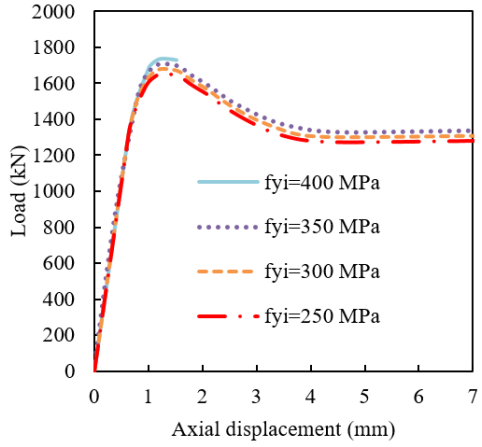

Figure 9. Influence of inner tube yield strength on the column capacity

In terms of the influence of concrete strength on the response of R-CFDST columns, as shown in Fig. 7, the results indicate that higher-strength concrete significantly enhances both the load capacity and the initial stiffness of the column. When the concrete strength increases from 30 MPa to 60 MPa, the ultimate capacity increases by up to 42.6%. This suggests that the use of high-strength concrete is an effective approach to enhancing the load-bearing capacity. These results are consistent with previous studies regarding the influence of concrete strength on R-CFDST column performance.

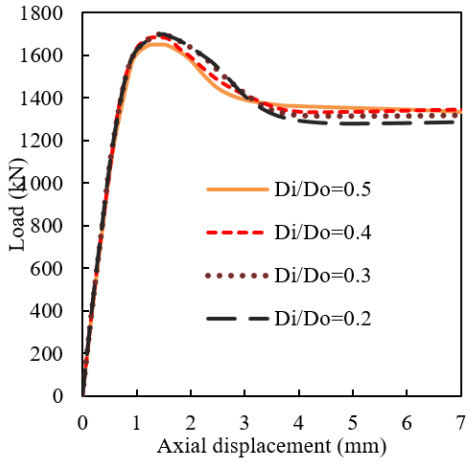

Figure 10. Influence of the column's hollow ratio on the column capacity

Similarly, when considering the influence of both the inner and outer steel tube strengths on the load-bearing capacity of R-CFDST columns, Figs. 8 and 9 show that increasing the strength of the outer steel tube only slightly improves the column's initial stiffness. However, the stiffness does not change noticeably after the peak load is reached. Furthermore, increasing the outer steel tube strength from 250 MPa to 400 MPa significantly enhances the column's load-bearing capacity by up to 17.82%. Nevertheless, this effect becomes insignificant when higher-strength inner steel tubes are used.

Regarding the effect of the column hollow ratio, Fig. 10 demonstrates that this ratio has only a small effect on both the strength and stiffness of R-CFDST columns when it is increased from 0.2 to 0.5. This is due to the substantial confinement provided by the reinforced concrete infill. This implies that, for R-CFDST columns, the use of longitudinal reinforcement can significantly reduce the column weight while its capacity is only slightly reduced, highlighting the notable contribution of longitudinal reinforcement to the performance of CFDST columns.

5. Evaluation of theoretical predictions for the ultimate load in R-CFDST columns

To evaluate the accuracy of standards and existing formulations for calculating the ultimate load capacity of R-CFDST columns presented in Table 1 of Section 2, results obtained from these modified formulations are compared with those obtained from FE models of 29 R-CFDST circular columns as shown in Table 3. The geometric parameters, material properties, and longitudinal reinforcement ratio were considered in 7 groups: longitudinal reinforcement ratio (samples R1-R5), concrete compressive strength (samples R6-R9), external steel tube yield strength (samples R10-R13), internal steel tube yield strength (samples R14-R17), D_o/t_o ratio (R18-R21), D_i/t_i ratio (samples R22-R25), and D_i/D_o ratio (samples R26-R29). Fig. 11 indicates the comparison of the ultimate loads obtained from modified formulations and FE results for 29 case studies. It can be seen from this figure that the predictive results from the modified equations show a discrepancy with FE results with a variation of approximately 10%. In particular, it is apparent that the ACI 318-14 [2] and AISC 360-22 [3] standards provide a conservative prediction of the ultimate load of the R-CFDST columns. This is due to the fact that these standards did not consider the confinement effect in the concrete core. In contrast, formulae suggested by Eurocode 4 [1], Han et al. [17], and Yu et al. [14] slightly overestimate the ultimate load of the column. On the other hand, it can be observed that the ultimate loads obtained from the modified equation of Hassanein et al. [15] closely match those obtained from FE results in almost case studies. This emphasizes the accuracy of the modified equation of Hassanein et al.

[15] and this equation can be employed for the practical design of R-CFDST columns under uniaxial compression.

Table 3. Comparison of the ultimate load between the modified formulations and FE results for R-CFDST columns

No.	Specimen	D_o (mm)	t_o (mm)	D_i (mm)	t_i (mm)	L (mm)	f_c (MPa)	f_{yo} (MPa)	f_{yi} (MPa)	d_r (mm)	n_r	η_r (%)	P_{FE} (kN)	P_{ACI} (kN)	P_{EC4} (kN)	P_{AISC} (kN)	P_{Han} (kN)	P_{Yu} (kN)	$P_{Hanssanein}$ (kN)
1	R1	180	3	60	3	500	40	275	350	0	0	0.00%	1451.0	1359.1	1545.2	1442.9	1542.6	1557.5	1516.8
2	R2	180	3	60	3	500	40	275	350	6	6	0.73%	1608.1	1427.1	1613.2	1510.9	1610.6	1625.5	1584.8
3	R3	180	3	60	3	500	40	275	350	8	6	1.30%	1661.2	1479.9	1666.0	1563.7	1663.4	1678.3	1637.6
4	R4	180	3	60	3	500	40	275	350	10	6	2.04%	1710.6	1547.5	1733.6	1631.3	1731.0	1745.9	1705.2
5	R5	180	3	60	3	500	40	275	350	12	6	2.93%	1793.0	1630.7	1816.8	1714.5	1814.2	1829.1	1788.4
6	R6	180	3	60	3	500	30	275	350	10	6	2.04%	1513.3	1369.4	1534.4	1432.3	1516.3	1569.9	1512.0
7	R7	180	3	60	3	500	40	275	350	10	6	2.04%	1710.6	1547.5	1733.6	1631.3	1731.0	1745.9	1705.2
8	R8	180	3	60	3	500	50	275	350	10	6	2.04%	1943.3	1725.6	1934.2	1830.4	1945.7	1921.9	1898.3
9	R9	180	3	60	3	500	60	275	350	10	6	2.04%	2159.1	1903.7	2138.0	2029.4	2160.4	2097.9	2091.5
10	R10	180	3	60	3	500	40	250	350	10	6	2.04%	1669.0	1505.8	1687.0	1589.6	1685.9	1685.4	1656.0
11	R11	180	3	60	3	500	40	300	350	10	6	2.04%	1747.3	1589.2	1779.8	1673.0	1776.1	1806.4	1754.3
12	R12	180	3	60	3	500	40	350	350	10	6	2.04%	1835.0	1672.6	1870.7	1756.4	1866.2	1927.4	1852.7
13	R13	180	3	60	3	500	40	400	350	10	6	2.04%	1918.3	1756.0	1959.9	1839.8	1956.3	2048.4	1951.1
14	R14	180	3	60	3	500	40	275	250	10	6	2.04%	1653.9	1493.8	1690.1	1577.6	1677.3	1692.2	1647.1
15	R15	180	3	60	3	500	40	275	300	10	6	2.04%	1682.3	1520.7	1711.8	1604.5	1704.1	1719.1	1676.1
16	R16	180	3	60	3	500	40	275	350	10	6	2.04%	1710.6	1547.5	1733.6	1631.3	1731.0	1745.9	1705.2
17	R17	180	3	60	3	500	40	275	400	10	6	2.04%	1738.5	1574.4	1755.6	1658.2	1757.9	1772.8	1734.2
18	R18	180	2	60	3	500	40	275	350	10	6	2.04%	1558.4	1415.0	1572.3	1501.0	1563.6	1545.4	1542.6
19	R19	180	3	60	3	500	40	275	350	10	6	2.04%	1710.6	1547.5	1733.6	1631.3	1731.0	1745.9	1705.2
20	R20	180	4	60	3	500	40	275	350	10	6	2.04%	1862.9	1678.5	1894.9	1760.1	1903.3	1943.8	1858.0
21	R21	180	5	60	3	500	40	275	350	10	6	2.04%	2014.8	1808.0	2054.2	1887.5	2080.7	2138.9	2007.9
22	R22	180	3	60	2	500	40	275	350	10	6	2.05%	1644.9	1487.0	1684.0	1570.8	1670.5	1683.9	1634.3
23	R23	180	3	60	3	500	40	275	350	10	6	2.04%	1710.6	1547.5	1733.6	1631.3	1731.0	1745.9	1705.2
24	R24	180	3	60	4	500	40	275	350	10	6	2.02%	1775.5	1605.8	1781.9	1689.6	1789.3	1805.7	1775.9
25	R25	180	3	60	5	500	40	275	350	10	6	2.01%	1841.4	1661.9	1828.6	1745.7	1845.4	1863.2	1845.9
26	R26	180	3	36	3	500	40	275	350	8	8	1.63%	1693.3	1502.3	1719.5	1593.3	1701.6	1715.6	1673.3
27	R27	180	3	54	3	500	40	275	350	8	8	1.70%	1700.9	1518.4	1713.0	1604.3	1706.6	1721.4	1680.4
28	R28	180	3	72	3	500	40	275	350	8	8	1.83%	1684.3	1517.2	1684.6	1596.0	1689.8	1704.8	1664.3
29	R29	180	3	90	3	500	40	275	350	8	8	2.02%	1648.8	1498.7	1633.1	1568.4	1651.2	1665.8	1625.5

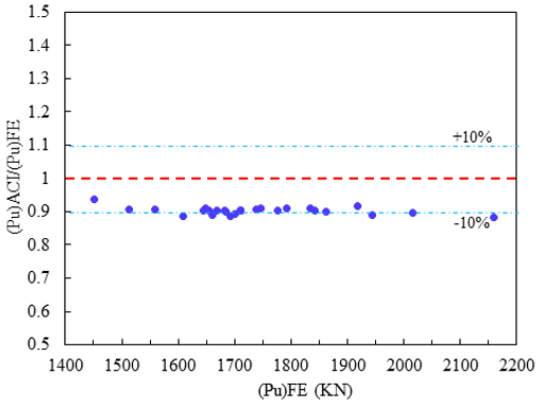

(a) ACI 318-14 [2]

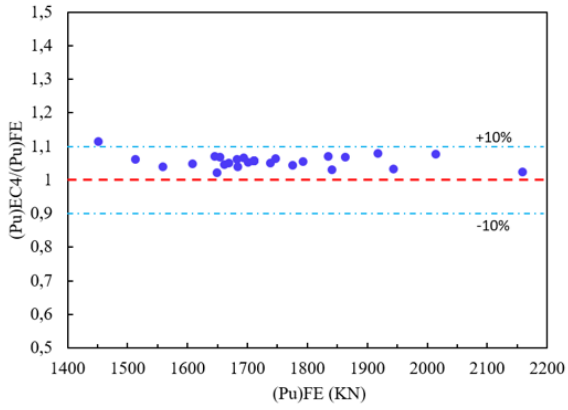

(b) Eurocode 4 [1]

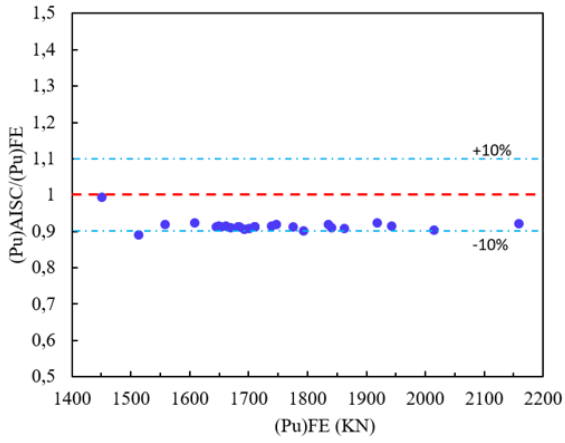

(c) AISC 360-22 [3]

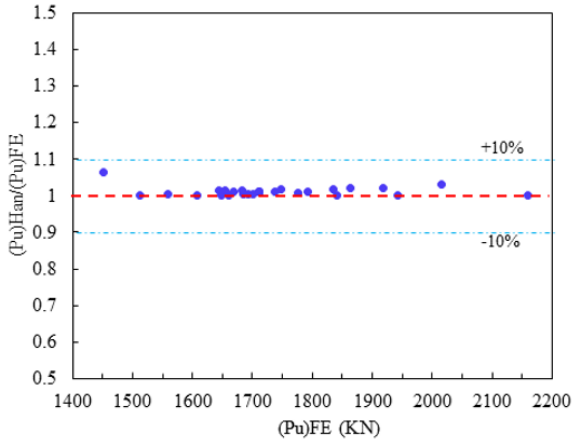

(d) Han et al. [17]

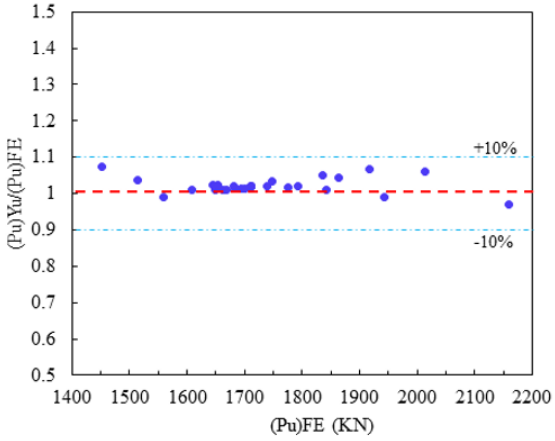

(e) Yu et al. [14]

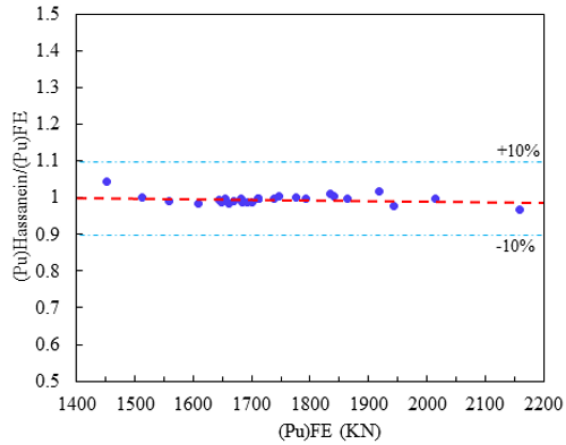

(f) Hassanein et al. [15]

Figure 11. Comparison of the ultimate load between the modified formulations and FE results

6. Conclusions

This paper presents a numerical investigation of the load-bearing capacity of reinforced concrete-filled double-skin steel tube (R-CFDST) circular columns under axial compression. Some conclusions can be drawn as follows:

- FE models for CFST, R-CFST, and CFDST columns were developed, and their accuracy was verified by comparing with experimental results. The models showed a good agreement in terms of both the ultimate load and the axial load – displacement response. A validated FE model was subsequently employed to simulate R-CFDST columns using the same modeling procedure.

- A parametric study was conducted to examine the influences of key parameters on the axial capacity of R-CFDST columns. It was demonstrated that the longitudinal reinforcement ratio, concrete compressive strength, and yield strength of the outer steel tube significantly influence the column's load capacity. In contrast, the yield strength of the inner steel tube and the column hollow ratio have minimal effects.

- It was found that when the longitudinal reinforcing bar ratio increases from 0% to 2.93%, the ultimate capacity of the column remarkably increases by up to 17.91%. This highlights the importance

of the longitudinal reinforcing bars in the concrete core.

- The ultimate loads obtained from the validated FE models were compared with predictions from various design codes and analytical models. It was found that the ACI 318-14 [2] and AISC 360-22 [3] standards underestimate the column capacity, while Eurocode 4 [1] overestimates it. The formulae proposed by Han et al. [17] and Yu et al. [14] slightly overestimate the column capacity. Among all considered formulations, a modified equation by Hassanein et al. [15] provided the best prediction of the ultimate load of the R-CFDST column under uniaxial compression.

Acknowledgements

This research is funded by Vietnam National Foundation for Science and Technology Development (NAFOSTED) under grant number 107.01-2023.63.

References

[1] Eurocode 4 Part 1-1 (2004). *Design of Composite Steel and Concrete Structures - Part 1-1: General Rules and Rules for Buildings*. European Committee for Standardization, Brussels.

[2] ACI 318-14 (2014). *Building code requirements for structural concrete and commentary*. American Concrete Institute, Detroit, USA.

[3] ANSI/AISC 360-22 (2022). *Specification for Structural Steel Buildings*. American Institute of Steel Construction, Chicago, USA.

[4] Gardner, N. J., Jacobson, E. R. (1967). Structural Behavior of Concrete Filled Steel Tubes. *ACI Journal Proceedings*, 64(7):404–413.

[5] Schneider, S. P. (1998). Axially Loaded Concrete-Filled Steel Tubes. *Journal of Structural Engineering*, 124(10):1125–1138.

[6] Uy, B. (2000). Strength of Concrete Filled Steel Box Columns Incorporating Local Buckling. *Journal of Structural Engineering*, 126(3):341–352.

[7] Vu, Q.-V., Truong, V.-H., Thai, H.-T. (2021). Machine learning-based prediction of CFST columns using gradient tree boosting algorithm. *Composite Structures*, 259:113505.

[8] Tran, V.-L., Thai, D.-K., Kim, S.-E. (2019). Application of ANN in predicting ACC of SCFST column. *Composite Structures*, 228:111332.

[9] Zarringol, M., Thai, H.-T., Naser, M. Z. (2021). Application of machine learning models for designing CFCFST columns. *Journal of Constructional Steel Research*, 185:106856.

[10] Viet, V. Q., Ha, H., Hoan, P. T. (2019). Evaluation of ultimate bending moment of circular concrete-filled double skin steel tubes using finite element analysis. *Journal of Science and Technology in Civil Engineering (STCE) - NUCE*, 13(1):21–32.

[11] Viet, V. Q., Hung, T. V., Hoan, P. T. (2019). Investigation of ultimate bending moment of circular concrete-filled double skin steel tubes with joint connection using finite element analysis. *Journal of Science and Technology in Civil Engineering*, 13(4V):115–128. (in Vietnamese).

[12] Uenaka, K., Kitoh, H., Sonoda, K. (2010). Concrete filled double skin circular stub columns under compression. *Thin-Walled Structures*, 48(1):19–24.

[13] Han, L.-H., Li, Y.-J., Liao, F.-Y. (2011). Concrete-filled double skin steel tubular (CFDST) columns subjected to long-term sustained loading. *Thin-Walled Structures*, 49(12):1534–1543.

[14] Yu, M., Zha, X., Ye, J., Li, Y. (2013). A unified formulation for circle and polygon concrete-filled steel tube columns under axial compression. *Engineering Structures*, 49:1–10.

[15] Hassanein, M. F., Kharoob, O. F., Liang, Q. Q. (2013). Circular concrete-filled double skin tubular short columns with external stainless steel tubes under axial compression. *Thin-Walled Structures*, 73:252–263.

[16] Pagoulatou, M., Sheehan, T., Dai, X. H., Lam, D. (2014). Finite element analysis on the capacity of circular concrete-filled double-skin steel tubular (CFDST) stub columns. *Engineering Structures*, 72: 102–112.

[17] Han, L.-H., Ren, Q.-X., Li, W. (2011). Tests on stub stainless steel–concrete–carbon steel double-skin tubular (DST) columns. *Journal of Constructional Steel Research*, 67(3):437–452.

[18] Hassanein, M. F., Kharoob, O. F. (2014). Compressive strength of circular concrete-filled double skin tubular short columns. *Thin-Walled Structures*, 77:165–173.

[19] Liang, Q. Q. (2009). Performance-based analysis of concrete-filled steel tubular beam–columns, Part I: Theory and algorithms. *Journal of Constructional Steel Research*, 65(2):363–372.

[20] Tang, J., Hino, S., Kuroda, I., Ohta, T. (1996). Modeling of Stress-Strain Relationships for Steel and Concrete in Concrete Filled Circular Steel Tubular Columns. *Steel Construction Engineering*, 3(11): 35–46.

[21] Han, L.-H., Yao, G.-H., Tao, Z. (2007). Performance of concrete-filled thin-walled steel tubes under pure torsion. *Thin-Walled Structures*, 45(1):24–36.

[22] Le, D.-N., Pham, T.-H., Pham, T.-D., Kong, Z., Papazafeiropoulos, G., Vu, Q.-V. (2024). An efficient long short-term memory-based model for prediction of the load-displacement curve of concrete-filled double-skin steel tubular columns. *Construction and Building Materials*, 449:138122.

[23] Le, T. T., Patel, V. I., Liang, Q. Q., Huynh, P. (2021). Axisymmetric simulation of circular concrete-filled double-skin steel tubular short columns incorporating outer stainless-steel tube. *Engineering Structures*, 227:111416.

[24] Elchalakani, M., Patel, V. I., Karrech, A., Hassanein, M. F., Fawzia, S., Yang, B. (2019). Finite element simulation of circular short CFDST columns under axial compression. *Structures*, 20:607–619.

[25] Yan, X.-F., Zhao, Y.-G., Lin, S. (2021). Compressive behaviour of circular CFDST short columns with high- and ultrahigh-strength concrete. *Thin-Walled Structures*, 164:107898.

[26] Li, W., Cai, Y.-X. (2019). Performance of CFDST stub columns using high-strength steel subjected to axial compression. *Thin-Walled Structures*, 141:411–422.

[27] Hassanein, M. F., Elchalakani, M., Karrech, A., Patel, V. I., Daher, E. (2018). Finite element modelling of concrete-filled double-skin short compression members with CHS outer and SHS inner tubes. *Marine Structures*, 61:85–99.

[28] Xiamuxi, A., Liu, C., Jierula, A. (2023). Study of the longitudinal reinforcement in reinforced concrete-filled steel tube short column subjected to axial loading. *Steel and Composite Structures*, 47(6):709–728.

[29] Tao, Z., Han, L.-H., Zhao, X.-L. (2004). Behaviour of concrete-filled double skin (CHS inner and CHS outer) steel tubular stub columns and beam-columns. *Journal of Constructional Steel Research*, 60(8): 1129–1158.

[30] Ekmekyapar, T., Alwan, O. H., Hasan, H. G., Shehab, B. A., AL-Eliwi, B. J. M. (2019). Comparison of classical, double skin and double section CFST stub columns: Experiments and design formulations. *Journal of Constructional Steel Research*, 155:192–204.

[31] Ekmekyapar, T., Ghanim Hasan, H. (2019). The influence of the inner steel tube on the compression behaviour of the concrete filled double skin steel tube (CFDST) columns. *Marine Structures*, 66:197–212.